

# Analytical prediction of abnormal temporary overvoltages due to ground faults in MV networks

F.M. Gatta\*, A. Geri, S. Lauria, M. Maccioni

*Department of Electrical Engineering, University of Rome "La Sapienza", Via Eudossiana n° 18, 00184 Roma, Italy*

Received 22 November 2005; received in revised form 31 May 2006; accepted 28 September 2006

Available online 28 November 2006

## Abstract

The paper deals with the temporary overvoltages that build up in radial MV distribution networks following the inception of a 1-phase-to-ground fault. It will be demonstrated that, for extended cable/overhead MV distribution networks with ungrounded neutral, in case of low resistance faults at critical locations along overhead lines, the neutral voltage can reach very large values, significantly higher than 1 p.u. (up to 2.5 p.u.). The attendant temporary overvoltages on healthy phases can be very large, much higher than  $\sqrt{3}$  p.u. (up to 3.5 p.u.). Fault currents are also affected, reaching twice the value calculated with simplified methods, i.e. neglecting series impedances. Quick yet accurate analytical formulas for the prediction of maximum overvoltages, fault currents and critical fault distances are presented, together with their validation by detailed ATP-EMTP simulations. The results of a study on an existing Italian 15 kV–50 Hz extended mixed cable/overhead distribution network are finally presented and discussed.

© 2006 Elsevier B.V. All rights reserved.

*Keywords:* Temporary overvoltages; MV radial network; Neutral grounding; 1-Phase-to-ground fault

## 1. Introduction

European MV (3.3–33 kV) distribution networks have various topologies, but radial operation with the provision for back-feed is widespread. In comparison to meshed operation, this practice allows simpler control and cheaper system protection but, on the other hand, it decreases the security of supply for MV customers and MV/LV distribution networks. Neutral grounding practices in Europe differ widely on a national basis (and sometimes within the same country), mainly due to historical and economical factors. Solutions adopted by distributors range from solidly grounded neutral (e.g. UK) to ungrounded neutral (e.g. Italy, parts of Finland and Spain), and include all kinds of impedance grounding or resonant grounding. In Italy the majority of public MV networks is currently operated with ungrounded neutral, but a complete conversion to compensated grounding is envisaged in the mid-term.

Temporary overvoltages originated by 1-phase-to-ground (1- $\Phi$ -to-Gr) faults are among the most important consequences

of the neutral grounding practice. When calculating 1- $\Phi$ -to-Gr fault currents and overvoltages in networks with ungrounded or high impedance-grounded neutral, line series impedances are usually neglected. This approximation was justified when dealing with small distribution networks, consisting of mostly overhead lines. Today, MV networks can be relatively large (200–400 km of aggregate line length) consisting mostly of cables, with long overhead and mixed cable/overhead lines in suburban areas. For such networks and in case of ungrounded neutral, neglecting line series impedances can lead to unacceptable underestimation of 1- $\Phi$ -to-Gr fault currents and overvoltages.

The above simplification yields maximum healthy phase temporary overvoltages just a little larger than the phase-to-phase nominal voltage ( $\sqrt{3}$  p.u. to ground), i.e. 1.823 p.u. with ungrounded neutral [1], for the critical fault resistance value  $R_F = 0.124/(\omega C_{0N})$ .

On the contrary, larger overvoltages are actually recorded in real networks: with ungrounded neutral, critical but credible network configurations in case of 1- $\Phi$ -to-Gr fault are liable to experience healthy phases' overvoltages over 3 p.u. [8]. Such overvoltages can cause insulation failure at weak points of the healthy phases, thus leading to a double fault

\* Corresponding author. Tel.: +39 06 44585805; fax: +39 06 4883235.  
E-mail address: [fabiomassimo.gatta@uniroma1.it](mailto:fabiomassimo.gatta@uniroma1.it) (F.M. Gatta).

to ground (as often recorded by MV line protection systems). Furthermore, double faults in ungrounded neutral networks, often imputed to intermittent arcs to ground, could be indeed explained in terms of the above described fault-originated overvoltages.

In this paper, the calculation of 1- $\Phi$ -to-Gr fault quantities for ungrounded or impedance-grounded networks is reappraised, leading to simple and accurate closed-form analytical expressions for fault currents and, notably, for temporary overvoltages.

Formulas have been validated by detailed ATP-EMTP simulation of an existing Italian 15 kV–50 Hz extended mixed cable/overhead line distribution network.

## 2. Temporary overvoltages in extended MV distribution network

### 2.1. Basic considerations

In order to avoid underestimating 1- $\Phi$ -to-Gr low-resistance fault current [2–4] and attendant temporary overvoltages in ungrounded neutral networks, the longitudinal impedance of the faulted line must be taken into account. In fact, at critical fault locations, the ratio between zero-sequence and positive-sequence reactances, though still negative, can assume relatively small absolute values (e.g. <10), thus, approaching a resonant region [6,8]. From the physical point of view, the increase of the healthy phases voltage at fault point and, even more, at the MV supply busbars, is due to the marked Ferranti effect engendered by the relatively high capacitive fault current flowing in the inductive series line impedances.

In the following, it will be evidenced that, in case of 1- $\Phi$ -to-Gr bolted fault, neutral and healthy phases voltages may attain 1.5–2.5 and 2.5–3.5 p.u., respectively. Moreover, fault currents are also significantly greater than those yielded by simplified calculations, raising concerns about touch and step voltages at the fault point.

The phenomenon causing these high overvoltages has been pointed out in the first half of the 20th century, in the developing stage of HV transmission and subtransmission systems [4,5] which, today, are in general effectively grounded [6]. The next sections show that this phenomenon also occurs in large, ungrounded neutral MV networks. Moreover, the sequence component network analysis and proposed formulas can be also applied to impedance-grounded and resonant-grounded networks, especially in order to predict system response during critical compensation contingencies (e.g. large mismatch and/or loss of compensation devices).

### 2.2. Sequence component network analysis

Let us consider the MV distribution network shown in Fig. 1, consisting of many overhead/cable radial lines originating from the MV busbars (B) of the primary substation (PS), which is supplied by a HV/MV step-down transformer with ungrounded neutral (switch S open in Fig. 1a).

In case of 1- $\Phi$ -to-Gr fault at receiving end of a radial line, the fault current  $I_F$  and the healthy phases' voltages are evaluated by solving the circuit of Fig. 1b. The positive/negative sequence impedance of the HV/MV step-down transformer,  $Z_{1NTR}$ , can be neglected in comparison with the series impedances of the faulted line,  $Z_{1fl}$ . Considering the zero-sequence capacitance of the faulty line connected to the MV busbars, the circuit of Fig. 1c is then arrived at. The latter approximation is certainly acceptable in case of a large MV network, as in the case under consideration. Solving the circuit of Fig. 1c the following expressions are found:

$$I_F = \frac{3E}{2R_{1fl} + R_{0fl} + 3R_F + j(2X_{1fl} + X_{0fl} - 1/(\omega C_{0N}))} \quad (1)$$

$$E_{0F} = -\frac{R_{0fl} + j(X_{0fl} - 1/(\omega C_{0N}))}{2R_{1fl} + R_{0fl} + 3R_F + j(2X_{1fl} + X_{0fl} - 1/(\omega C_{0N}))} E \quad (2)$$

$$E_{0B} = \frac{-1/(j\omega C_{0N})}{2R_{1fl} + R_{0fl} + 3R_F + j(2X_{1fl} + X_{0fl} - 1/(\omega C_{0N}))} E \quad (3)$$

$$E_{TB} = \left[ \frac{-1/(j\omega C_{0N})}{2R_{1fl} + R_{0fl} + 3R_F + j(2X_{1fl} + X_{0fl} - 1/(\omega C_{0N}))} + (1\angle 120^\circ) E \right] \quad (4)$$

The latter can be also written as

$$E_{TB} = \left[ \frac{jE}{[(2r_{1fl} + r_{0fl}) + j(2x_{1fl} + x_{0fl})]L_F I_{0C} + 3R_F I_{0C} - jE} + (1\angle 120^\circ) E \right] \quad (5)$$

Eqs. (1)–(5) point out to several interesting results:

- Increasing the distance of the fault from the MV busbars, the magnitude of  $I_F$  yielded by (1) has a maximum at a given distance (see Appendix B) and then decreases: in fact, the capacitive zero-sequence impedance is lowered by the inductive series reactance of the faulted line but the augmented series resistance of the same phase tends to increase the overall impedance. This behaviour is more marked in overhead MV lines, usually not equipped with shield wires, whose zero sequence reactance  $X_{0fl}$  can be three to four times the positive sequence reactance  $X_{1fl}$ . For MV cables with grounded screen/armour the increase of  $I_F$  is small, because frequently it is  $X_{0fl} \leq X_{1fl}$  and  $R_{0fl} > R_{1fl}$ .
- The magnitude of zero-sequence voltage at fault point,  $E_{0F}$ , can be higher than 1 p.u., due to the Ferranti effect of the capacitive fault current,  $I_{0F}$ , flowing in the positive and negative sequence inductive line impedances (Fig. 1c). It also follows that negative and positive sequence voltages have amplitudes greater than 1 and 0 p.u., respectively. The corresponding voltage of the healthy phases can be significantly higher than  $\sqrt{3}$  p.u.

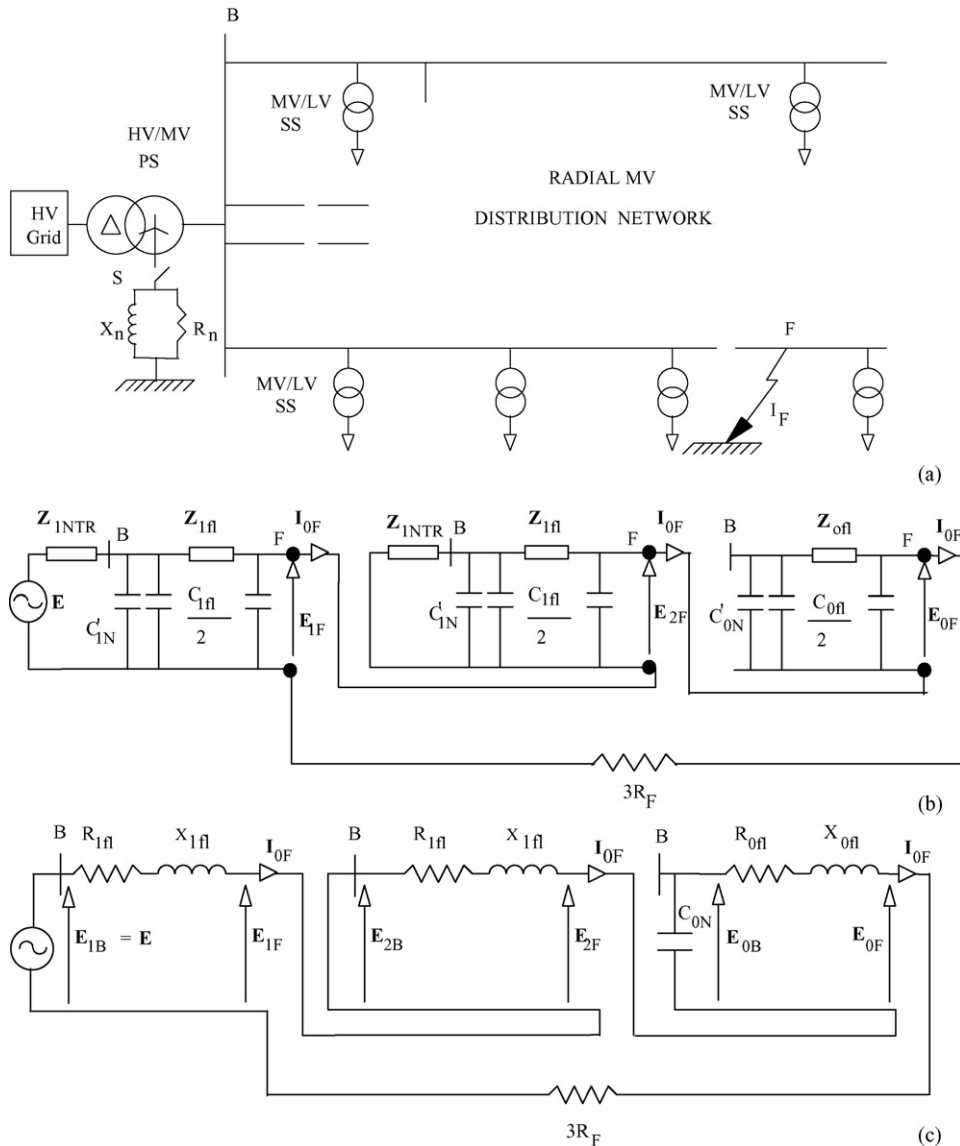


Fig. 1. Radial MV distribution network: (a) single-line diagram; (b) connection of sequence networks in case of 1- $\Phi$ -to-Gr fault at the end of a line; (c) equivalent circuit (see text for approximations).

- The zero sequence voltage magnitude at the PS busbars,  $E_{0B}$ , is even higher than  $E_{0F}$ , due to the Ferranti effect on the zero sequence faulted line impedance. The increase can be estimated at about 1–1.5 kV per 100 A of zero sequence fault current and 10 km of line length. As a consequence, at the MV busbars the healthy phase voltages may attain 2.5–3.5 p.u. with a faulted phase voltage over  $\sqrt{3}$  p.u.
- Fault current and voltages are very sensitive to fault and line resistances. A fault resistance,  $R_F$ , of some tens of Ohms drastically reduces fault current and overvoltages.
- The critical fault distance from PS busbars,  $L_{Pmax}$ , corresponding to the maximum overvoltages on healthy phases, depends on the network size (i.e. on  $C_{0N}$ ) and on  $R_F$ . Equations yielding the fault distances,  $L_{0max}$  and  $L_{Pmax}$ , that in turn maximize  $I_F$ ,  $E_{0B}$  and  $E_{TB}$ , and the fault resistance,  $R_F$ , that engenders the maximum healthy phases busbars overvoltage are given in the Appendix B.

2.3. MV network with ungrounded neutral: a test case

The above phenomena can be quantified by considering the simple 20 kV–50 Hz radial distribution network of Fig. 2, including 170 km of overhead lines ( $r_1 + jx_1 = 0.23 + j0.35 \Omega/\text{km}$ ;

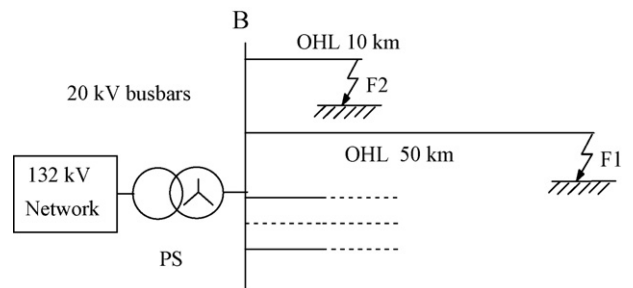


Fig. 2. 20 kV–50 Hz radial network (80 km cable plus 170 km OHLs).

Table 1  
Fault current and overvoltage for 1- $\Phi$ -to-Gr faults in 20 kV ungrounded neutral network of Fig. 2

Fault location		$I_F = 3 I_{0F}$ (A)	Voltages at	$E_0$ (p.u.)	$E_R$ (p.u.)	$E_S$ (p.u.)	$E_T$ (p.u.)
F1	$R_F = 0 \Omega$	528	Fault point	1.34	0	1.78	2.52
			PS busbars	2.43	1.78	2.47	3.39
	$R_F = 25 \Omega$	270	Fault point	0.70	0.58	0.89	1.81
			PS busbars	1.24	1.24	1.04	2.24
F2	$R_F = 0 \Omega$	251	Fault point	1.05	0	1.77	1.83
			PS busbars	1.16	0.17	1.83	1.90
	$R_F = 25 \Omega$	216	Fault point	0.89	0.47	1.35	1.85
			PS busbars	0.99	0.53	1.39	1.92

$r_0 + jx_0 = 0.376 + j1.48 \Omega/\text{km}$ ,  $c_0 = 4.5 \text{ nF}/\text{km}$ ) and 80 km of underground cable lines ( $c_0 = 240 \text{ nF}/\text{km}$ ).

Two 1- $\Phi$ -to-Gr fault locations are considered: at the end of a 10 km long overhead line (OHL), or at the end of a 50 km long overhead line (i.e. F1 and F2 in Fig. 2).

Table 1 reports voltages and currents for fault locations F1 and F2, with fault resistance  $R_F = 0$  and  $25 \Omega$ .

The 1- $\Phi$ -to-Gr fault (R-phase) at the end of the 50 km long line with  $R_F = 0 \Omega$  causes a very high overvoltage, up to 3.4 p.u. on T-phase of PS busbars; at fault location the overvoltage on the same phase reaches 2.52 p.u. With a  $25 \Omega$  fault resistance, the overvoltages are reduced to 2.24 and 1.81 p.u., respectively. If the 1- $\Phi$ -to-Gr fault occurs at receiving end of the 10 km long overhead line, maximum overvoltages, found with  $R_F = 25 \Omega$ , are lower: 1.92 and 1.85 p.u., respectively, at PS busbars and fault location.

Very large neutral overvoltages may occur at PS busbars and at every healthy MV line, ranging from 1.24 to 2.43 p.u. when  $R_F$  is between 0 and  $25 \Omega$ .

Note that for faults near PS busbars, the maximum overvoltages are found for  $R_F \neq 0 \Omega$  (e.g. for the F2 fault, 10 km distant from the PS busbars, 1.96 p.u. would occur for  $R_F = 13.4 \Omega$ ). For distant faults, i.e., at the end of long lines, the maximum overvoltages occur when  $R_F = 0 \Omega$  (see Appendix B).

For bolted faults ( $R_F = 0 \Omega$ ),  $I_F$  at the end of long lines is far greater than the value yielded by the usual simplified calculation approach: e.g., in F1, it is of 528 A instead of 217 A. For short lines, the increase is smaller (up to 251 A in F2).

Table 1 shows also that, for faults far from the busbars, currents are markedly affected by  $R_F$ . For example,  $I_F$  at location F1 halves (from 528 to 270 A) with  $R_F$  increasing from 0 to  $25 \Omega$ , while at location F2, the corresponding decrease of  $I_F$  is only 15% (i.e. from 256 to 216 A).

Fig. 3 shows the maximum healthy phases' overvoltages at supply busbars, versus the fault distance, with  $R_F = 0 \Omega$  and for different values of the capacitive fault current  $I_{CF}$ , i.e. different overall network extensions. Note that  $E_{\max}$  on the healthy phases is the same (3.77 p.u.) for all network extensions: in fact, Eq. (5), shows that when  $R_F = 0 \Omega$ ,  $E_{\max}$  is a function of the product  $L_g I_{CF}$ ; it follows that in larger networks (i.e., with high  $I_{CF}$ ),  $E_{\max}$  is found for lower values of the fault distance.

Fig. 4 shows  $E_{\max}$  versus fault distance, for  $I_{CF} = 300 \text{ A}$  and  $R_F = 0, 5, \text{ and } 10 \Omega$ . For  $R_F = 10 \Omega$   $E_{\max}$  occurs for fault

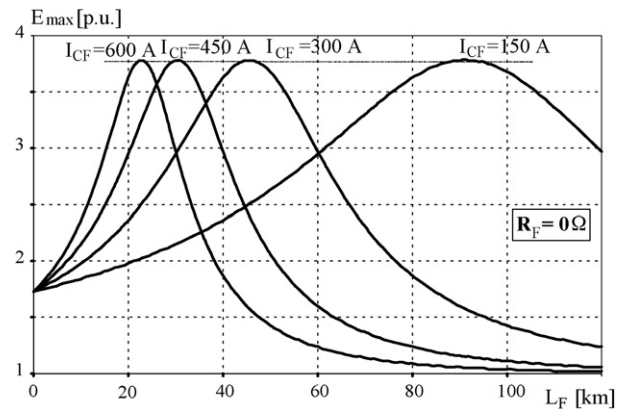


Fig. 3. Maximum healthy phases' overvoltages vs. fault distance from supply busbars ( $R_F = 0 \Omega$ ).

distances in the 40–45 km range and decreases from 3.77 to 2.66 p.u.

Fig. 5 shows that fault resistance reduces  $E_{\max}$  more effectively in large MV networks (as already stated). From Fig. 5 it can also be seen that, for credible values of network extension and fault resistances ( $I_{CF} = 300 \text{ A}$  and  $R_F = 5$  and  $10 \Omega$ -typical secondary substation grounding resistances-)  $E_{\max}$  can be very high, up to 2.6–3.15 p.u. for faults at the end of a 40 km overhead line.

Fig. 6 reports the “critical” fault distance  $L_{P_{\max}}$  (for healthy phase maximum overvoltages) versus capacitive fault current, for  $R_F$  ranging from 0 to  $50 \Omega$ . It can be noticed that  $L_{P_{\max}}$

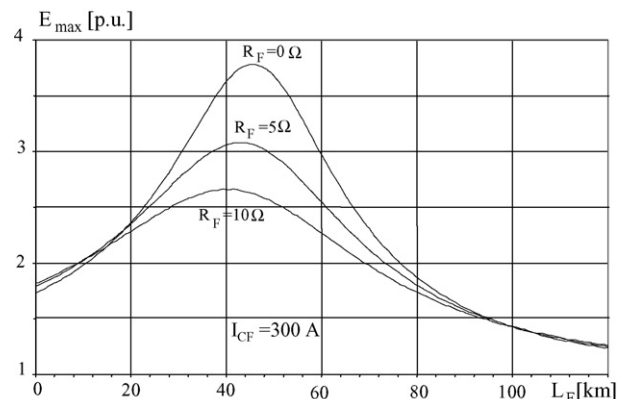


Fig. 4. Maximum healthy phases' overvoltages at busbars, vs. fault distance.

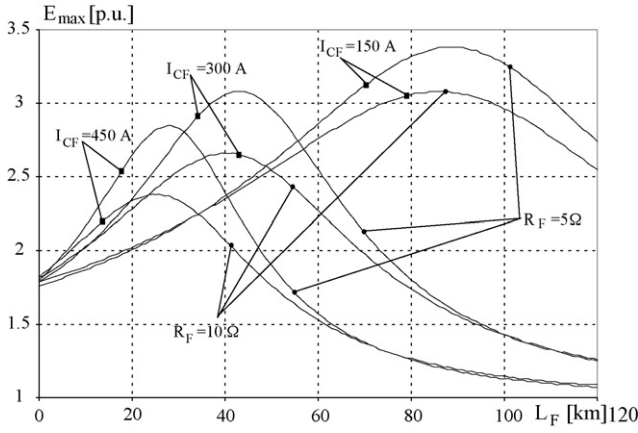


Fig. 5. Maximum healthy phases' overvoltage vs. fault distance, for several values of  $R_F$  and  $I_{CF}$ .

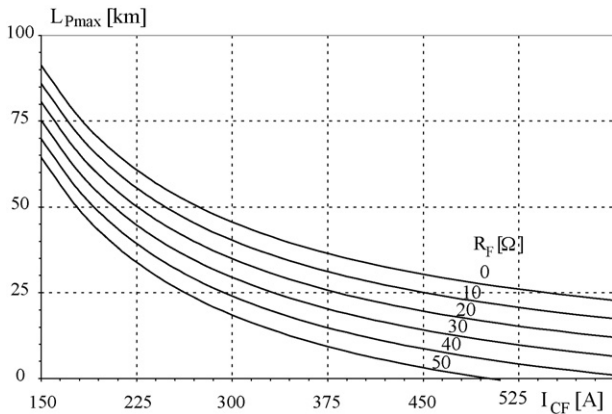


Fig. 6. Critical fault distance from supply busbars vs. capacitive fault current, for different values of fault resistance.

decreases with the increase of MV network extension and fault resistance. For high values of  $R_F$ , the maximum healthy phases' overvoltages occur in case of fault at the supply busbars.

Finally, maximum overvoltages,  $E_{max}$ , versus capacitive fault current are shown in Fig. 7 for various values of  $R_F$ .

Fig. 8 reports the vector diagrams of the voltages at fault point and at supply busbars, for a bolted 1-Φ-to-Gr fault at the receiving end of the 50 km long line.

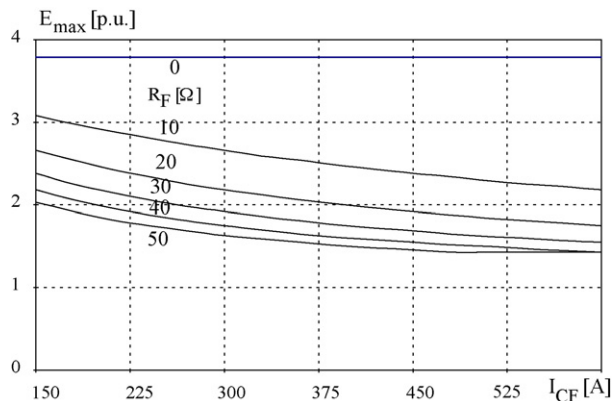


Fig. 7. Maximum healthy phases' overvoltages at supply busbars vs. capacitive fault current.

Fig. 8 shows that phase-to-phase voltages are strongly asymmetrical, with magnitudes greater than  $\sqrt{3}$  p.u., only at or near to the fault location. At the supply busbars and along healthy lines, phase-to-phase voltages are close to normal operating values and they are practically symmetrical.

MV windings of MV/LV distribution transformers are often delta-connected (e.g. in Italy); in this case, only transformers close to the fault may saturate, thus mitigating the overvoltages on healthy phases (the delta connection does not allow zero-sequence saturation). Saturation of voltage transformers, whose MV windings are connected in grounded wye, can mitigate the overvoltages. It should be pointed out that transformer saturation does not drastically limit the temporary overvoltages, because the voltage is in quadrature with the magnetic flux: when the flux is high (i.e. high current) the voltage is near zero.

The main causes of the overvoltage reduction are loads, additional losses related to increased voltages and magnetizing harmonics produced by core saturation. Detailed time-domain simulation is required in order to evaluate these effects, especially for complex network structures (e.g. ramified configurations of the long faulted cable/overhead mixed line).

#### 2.4. MV networks with compensated neutral: a test case

In Fig. 1 let us consider the switch S closed, so that the neutral is connected to ground by Petersen coil,  $X_n$ , and parallel resistance,  $R_n$ .  $X_n$  is chosen equal to  $1/(3\omega C_{0N})$  [3–7] while  $R_n$  is set in such a way to limit the resistive fault current at some tens of A (e.g. ENEL in Italy and EDF in France limit the resistive current to about 40 A and 20 A, respectively).

With the same approximations introduced in Section 2.1, and assuming an ideal perfect compensation of the zero-sequence network capacitances, solution of the circuit in Fig. 9 yields the following zero sequence voltages at fault point (6) and at supply busbars (7) in case of 1-Φ-to-Gr fault at the end of a radial line:

$$E_{0F} = -\frac{3R_n + R_{0ff} + jX_{0ff}}{2R_{1ff} + R_{0ff} + 3R_n + 3R_F + j(2X_{1ff} + X_{0ff})} E \quad (6)$$

$$E_{0B} = -\frac{-3R_n}{2R_{1ff} + R_{0ff} + 3R_n + 3R_F + j(2X_{1ff} + X_{0ff})} E \quad (7)$$

From (6) and (7) it follows that for bolted faults ( $R_F=0$ ) the amplitudes of  $E_{0B}$  and  $E_{0F}$  are less than 1 p.u.; since the neutral resistance  $R_n$  is prevalent, both above voltages are phase shifted by about  $180^\circ$  with respect to the pre-fault phase voltage  $E$ . Furthermore, as  $E_{1B}$ ,  $E_{1F}$ ,  $E_{2B}$ ,  $E_{2F}$  are very small, it can be concluded that the maximum overvoltages on healthy phases are not greater than  $\sqrt{3}$  p.u. for every fault location. For the network of Fig. 2, which requires  $X_n=53 \Omega$  and  $R_n=288 \Omega$  (resistive fault current  $\cong 40$  A), current and voltages for the fault at F2 (see Fig. 1) are reported in Table 2.

For bolted fault, the maximum neutral voltage is 0.97 p.u. at fault location, whereas the maximum healthy phase overvoltage, practically constant along each line, is not greater than 1.75 p.u..

For  $R_F=25 \Omega$  the above overvoltages decrease to 0.87–0.89 p.u. and to 1.66–1.68 p.u., respectively.

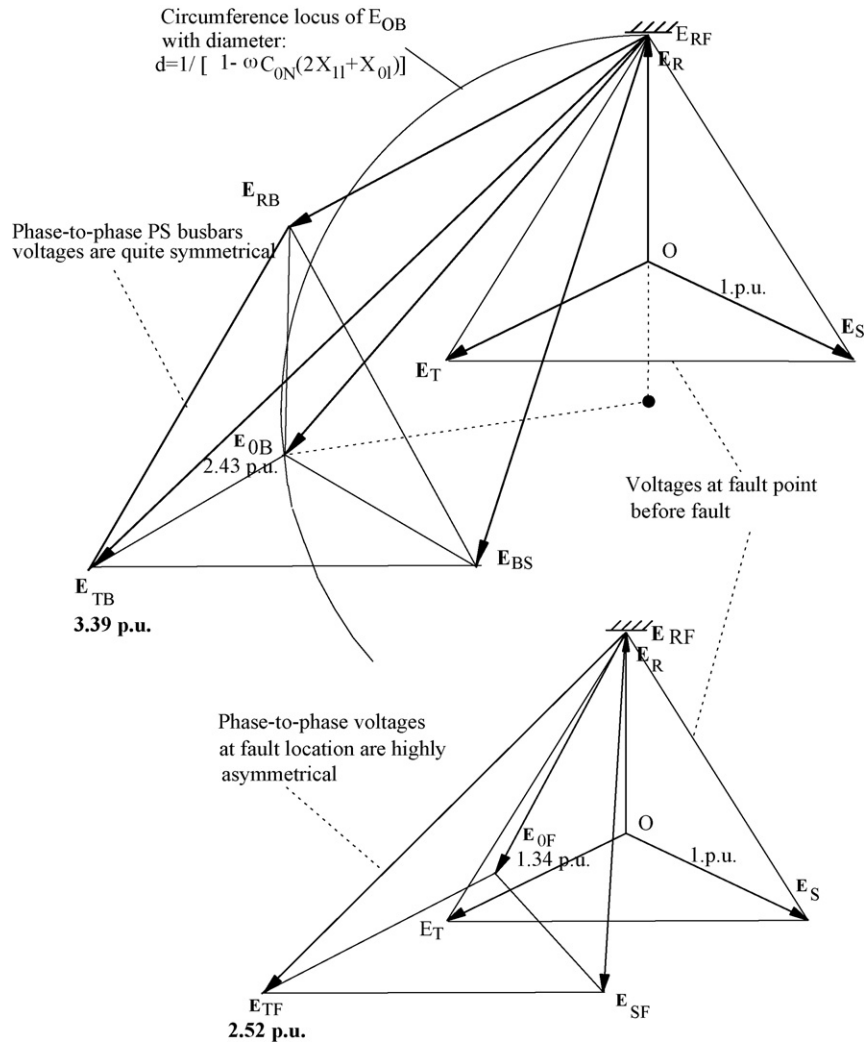


Fig. 8. Vector diagrams of the voltages at fault point and at supply busbars, in case of a 1- $\Phi$ -to-Gr bolted fault at the end of a 50 km long overhead line.

Table 2  
Fault current and voltages, in case of 1- $\Phi$ -to-Gr fault at location F2 of Fig. 2 network, with 100% compensated neutral

$R_F$ ( $\Omega$ )	$E_{0F}$ (p.u.)	$E_{TF}$ (p.u.)	$E_{0B}$ (p.u.)	$E_{TB}$ (p.u.)	$I_F$ (A)
0	$0.97 \angle 178^\circ$	$1.73 \angle 148^\circ$	$0.95 \angle 173^\circ$	$1.75 \angle 146^\circ$	$39.4 \angle -5.1^\circ$
25	$0.89 \angle 178^\circ$	$1.66 \angle 146^\circ$	$0.87 \angle 173^\circ$	$1.68 \angle 145^\circ$	$26.3 \angle -4.7^\circ$

### 3. 15 kV–50 Hz distribution network: a case study

An existing Italian 15 kV–50 Hz distribution network (Fig. 10) has been simulated by means of ATP-EMTP, in order to quantify the maximum temporary overvoltages which can occur following 1- $\Phi$ -to-Gr faults.

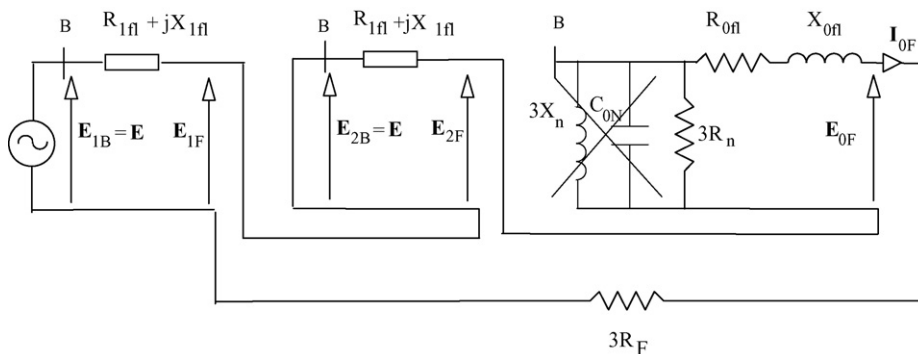


Fig. 9. Sequence networks connection in case of radial MV network with compensated neutral (100% compensation).

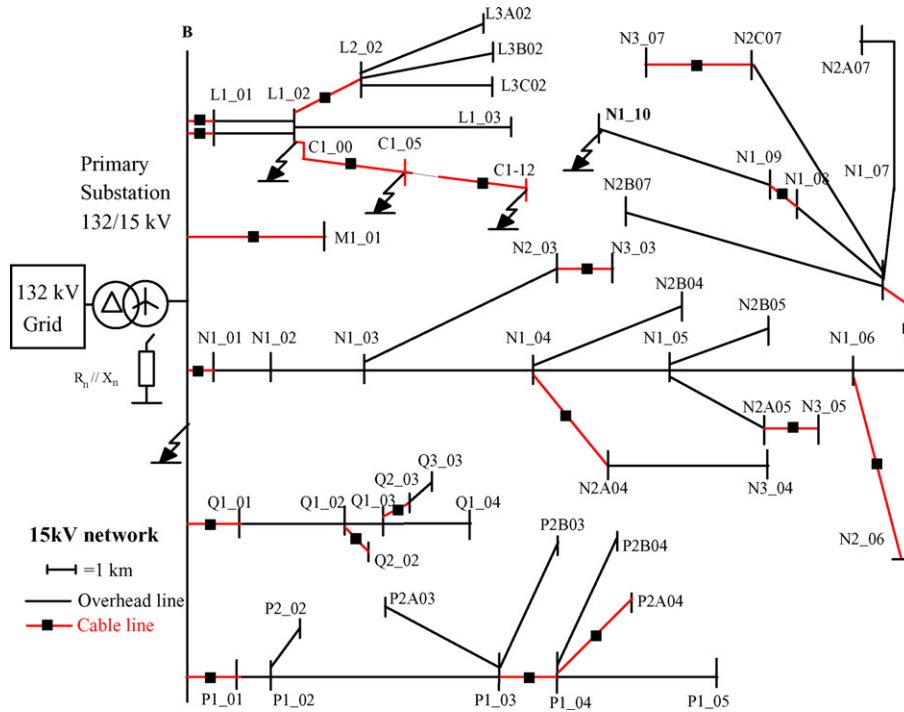


Fig. 10. Existing 15 kV–50 Hz Italian distribution network simulated with ATP-EMTP.

The 15 kV network, supplied by a 132/15 kV 25 MVA step-down transformer, has an overall line extension of 237 km, 73 km of which are cable lines. One of the five main radial mixed cable/overhead lines is 40 km long (from supply busbars to node N1\_10 in Fig. 10). A special very long cable line, whose screens/armours are connected to the buried ground wire (30 km from L1\_02 to C1\_12 in Fig. 10), is fed from a 15 kV switching substation of the first main radial line (B/L1\_03).

Two neutral grounding connections are analysed: ungrounded and grounded by a Petersen coil in paral-

lel with a resistance, (respectively, rated  $X_n = 83 \Omega$  and  $R_n = 280 \Omega$ -resistive fault current of 31 A-).

1- $\Phi$ -to-Gr faults were simulated by ATP-EMTP at every bus of the network but results are reported for the most relevant fault locations: supply busbars (bus B); line end of the 40 km long main mixed radial line (bus N1\_10); sending, mid point and receiving end of the 30 km long cable line (C1\_00, C1\_05, C1\_12), for the case of ungrounded neutral.

Table 3 shows the fault current and the maximum overvoltages occurring at supply busbars and in the above sections of the 30 km long cable line.

Table 3  
Fault current and overvoltages for 1- $\Phi$ -to-Gr faults in 15 kV network of Fig. 10, with ungrounded neutral

Fault point	B		N1_10		C1_00	C1_05	C1_12
Fault resistance, $R_F$ ( $\Omega$ )	0.5	1	5	30	–	–	–
Fault current, $I_F$ (A)	122	122	146	112	124	125	127
Maximum voltage (p.u.)							
CL00, B	1.76	1.76	2.37	2.00	1.76	1.79	1.82
CL04	1.76	1.76	2.37	2.00	1.76	1.79	1.82
CL12	1.76	1.76	2.38	2.00	1.76	1.79	1.82

Table 4  
Fault current and overvoltages for 1- $\Phi$ -to-Gr faults in the network of Fig. 10, with 100% compensated neutral

Fault point	B		N1_10		C1_00	C1_05	C1_12
Fault resistance, $R_F$ ( $\Omega$ )	0.5	1	5	30	–	–	–
Fault current, $I_F$ (A)	42	42	36	33	41	40	40
Maximum voltage (p.u.)							
CL00, B	1.74	1.74	1.71	1.66	1.74	1.74	1.74
CL04S	1.74	1.74	1.71	1.66	1.74	1.74	1.74
CL12S	1.74	1.71	1.71	1.67	1.76	1.74	1.74

Overvoltages up to 2.38 (2.00) p.u. are found for faults at the end of the 40 km long line with  $R_F = 5$  (30)  $\Omega$ . For the same case, Eq. (5) yields 2.33 (2.03) p.u. overvoltages. These values occur at supply busbars and in all healthy lines. The difference between the values obtained by ATP-EMTP and those calculated by analytical formulas is less than 2.2%. Faults at the end of the long cable line cause lower maximum overvoltages (1.82 p.u.), due to low zero sequence series reactance of the faulted cable line. A fault at the supply busbars engenders the lowest overvoltages (1.76 p.u.), practically equal to the phase-to-phase rated voltage.

The fault current is in the 112–146 A range, with the maximum value occurring for a fault at the end of the long overhead line: with  $R_F = 5 \Omega$  it is 20% greater than the fault current at the supply busbars. Fault currents in the long cable line do not practically change with fault position along the line.

Table 4 finally reports the results obtained for the case of compensated neutral. Fault current values are in the 33–42 A range, while maximum healthy phase overvoltages are limited to 1.74 p.u. (1.73 p.u. according to Eq. (5)) even for faults at the end of the long overhead line, as predicted. In this case the overvoltages at the supply busbars are in the 1.71/1.66 p.u. range, while Eq. (5) yields 1.68/1.61 p.u. overvoltages. The difference between the values obtained by ATP-EMTP and those calculated by analytical formulas is less than 3%.

#### 4. Conclusions

The paper dealt with the temporary overvoltages and fault current following 1- $\Phi$ -to-Gr faults in extended, mixed cable/overhead line, radial MV networks.

For networks with ungrounded neutral, it has been shown that:

- 1- $\Phi$ -to-Gr faults at the receiving end of long overhead lines can cause abnormal overvoltages, especially at Primary Substation busbars and in healthy lines.
- Overvoltages on neutral and healthy phases can reach values greater than 2.5/3.5 p.u., respectively, in case of bolted fault.
- For low resistance faults, maximum overvoltages do not occur at the fault point, but at the MV primary substation and at healthy lines: values obtained for an existing Italian 15 kV to 50 Hz radial network are in the 2.3–2.5 p.u. range.
- For a given MV network and fault resistance, there exists a critical fault distance which causes the maximum overvoltage on healthy phases.
- 1- $\Phi$ -to-Gr fault current increases with the distance of the fault from the MV primary substation; fault current magnitudes at remote locations can be significantly larger than those calculated with the usual approximations.

Analytical formulas, allowing quick and accurate evaluation of all quantities of interest (maximum overvoltages, fault currents and critical fault distances) have been arrived at.

The above phenomena and the presented formulas, have been respectively confirmed and validated by detailed ATP-EMTP simulation.

The paper also showed that, with compensated neutral, the above phenomena may be largely suppressed, as long as the compensation degree is near 100%. In the latter case the maximum overvoltages are not greater than  $\sqrt{3}$  p.u. However, the same phenomena highlighted for ungrounded neutral can be found also for compensated neutral networks, in case of partial or total failure of the neutral grounding impedance. Furthermore, in both cases of ungrounded and compensated neutral, special attention must be paid to evaluation of touch and step voltages, given the possible occurrence of earth fault currents larger than usually expected.

The authors are currently investigating the occurrence of abnormal phenomena in networks with imperfect neutral compensation (due to faults or changes in network structure).

#### Appendix A. List of symbols

$C_{0N}$	MV network zero-sequence capacitance
$C'_{1N}, C'_{0N}$	MV network positive-sequence and zero-sequence capacitance (minus the faulted line)
$C_{1ff}, C_{0ff}$	faulted line positive-sequence and zero-sequence capacitance
$E$	MV supply voltage
$E_{max}$	maximum healthy phases' overvoltage
$E_{TF}, E_{TB}$	T-phase voltage at fault location and at MV supply busbars
$E_{1B}, E_{2B}, E_{0B}$	positive-, negative-, and zero-sequence voltages at MV supply busbars
$E_{1F}, E_{2F}, E_{0F}$	positive-, negative-, and zero-sequence voltages at fault location
$I_{CF}, I_{0C}$	total and zero-sequence capacitive fault current (neglecting series impedances: $I_{CF} = 3I_{0C} = 3\omega C_{0N}E$ )
$I_F, I_{0F}$	fault current, zero-sequence fault current ( $=I_F/3$ )
$L_F$	fault distance from MV supply busbars
$L_{Pmax}$	critical fault distance from MV supply busbars (for healthy phase overvoltage at busbars)
$L_{0max}$	critical fault distance from MV supply busbars (for fault current and zero-sequence voltage at supply busbars)
$r_{1ff}, r_{0ff}, x_{1ff}, x_{0ff}$	positive-sequence and zero-sequence series resistances and reactances of the faulted line up to fault location, per unit length
$R_F$	fault resistance
$R_{1ff}, R_{0ff}, X_{1ff}, X_{0ff}$	positive-sequence and zero-sequence series resistances and reactances of the faulted line up to fault location
$X_n, R_n$	neutral grounding reactance (Petersen coil) and parallel resistance
$Z_{1ff}, Z_{0ff}$	positive-sequence and zero-sequence series impedances of the faulted line, up to fault location
$Z_{1NTR}, Z_{0NTR}$	HV/MV transformer positive-sequence and zero-sequence impedance

## Appendix B

In the following, practical formulas are given to evaluate quantities of interest in case of 1- $\Phi$ -to-Gr faults.

- Maximum overvoltage of the healthy phase at fault point is

$$E_{TF} = - \left[ \frac{[\sqrt{3}(R_{0f} + R_F) + 2X_{1f} + X_{0f} - 1/(\omega C_{0N})]}{2R_{1f} + R_{0f} + 3R_F + j(2X_{1f} + X_{0f} - 1/(\omega C_{0N}))} + j \frac{[\sqrt{3}(X_{0f} - 1/(\omega C_{0N})) - 2R_{1f} + R_{0f} - 3R_F]}{2R_{1f} + R_{0f} + 3R_F + j(2X_{1f} + X_{0f} - 1/(\omega C_{0N}))} \right] \frac{\sqrt{3}}{2} E \quad (B.1)$$

- Maximum values of  $I_F$  and  $E_{0B}$  occur for the fault distance from the supply busbars given by

$$L_{0max} = \frac{(2x_{1f} + x_{0f})/(\omega C_{0N}) - 3R_F(2r_{1f} + r_{0f})}{(2r_{1f} + r_{0f})^2 + (2x_{1f} + x_{0f})^2} \quad (B.2)$$

- Maximum overvoltage on healthy phases occurs for the fault distance given by

$$L_{Pmax} = - \frac{2/(\omega C_{0N}) + 3\sqrt{3}R_F}{\sqrt{3}R - X} + \frac{\sqrt{(A/\omega^2 C_{0N}^2) + (B/\omega C_{0N}) + C^2}}{\sqrt{R^2 + X^2}(\sqrt{3}R - X)} \quad (B.3)$$

where

$$R = 2r_{1f} + r_{0f}, \quad X = 2x_{1f} + x_{0f}, \quad C = 6RX; \quad A = 7R^2 + X^2 + 2\sqrt{3}RX; \quad B = 30RR_F X + 6\sqrt{3}X^2 R_F$$

- Maximum overvoltage on healthy Primary Substation phase occurs the for fault resistance given by

$$R_F = \frac{(2X_{1f} + X_{0f} - 2/(\omega C_{0N})) + \sqrt{(2X_{1f} + X_{0f} - 2/(\omega C_{0N}))^2 + 3(2X_{1f} + X_{0f} - 1/(\omega C_{0N}))^2}}{3\sqrt{3}} - \frac{2R_{1f} + R_{0f}}{3} \quad (B.4)$$

## References

- [1] IEEE Power Engineering Society, IEEE Guide for Application of Neutral Grounding in Electrical Utility Systems, Part IV—Distribution, IEEE Std. C62.92.4-1991, USA, 1992.
- [2] A. Augugliaro, A. Campoccia, L. Dusonchet, L'Energia Elettrica 5 (1989) 373–381.
- [3] A. Augugliaro, A. Campoccia, L. Dusonchet, L'Energia Elettrica 9 (1991) 217–225.
- [4] R. Willheim, M. Waters, Neutral Grounding in High-Voltage Transmission, Elsevier Publishing Company, 1956.
- [5] Westinghouse, Electrical Transmission and Distribution Reference Book, 4th ed., Pennsylvania, 1964.
- [6] IEEE Power Engineering Society, IEEE Guide for Application of Neutral Grounding in Electrical Utility Systems, Part I—Introduction, and Part V—Transmission System and Subtransmission System, IEEE Std. C62.92.1-2000 and IEEE Std. C62.92.5-1992.
- [7] V. Leitloff, L. Pierrat, R. Feuillet, ETEP—European Trans. on Electrical Power Engineering 4 (1994) 145–153.
- [8] P. Dimo, RGE—Revue Générale de l'Électricité 66 (1957) 297–306.

F.M. Gatta was born in Alatri (Italy) in 1956. In 1981 he received a doctor degree in Electrical Engineering from Rome University (Hons). He then joined the Rome University's Department of Electrical Engineering where he was appointed Researcher and in 1998 appointed Associate Professor in Electrical Power Systems. His main research interests are in the

field of power system analysis, long distance transmission, transient stability, temporary and transient overvoltages, series and shunt compensation, SSR, distributed generation, power plants, design, planning and operation of transmission and distribution network, unconventional distribution system.

A. Geri was born in Terni (Italy) in 1961. He received a University degree in Electrical Engineering from University of Rome “La Sapienza” in 1987. He began academic activity in 1989 as researcher of Electrical Science at University of Rome “La Sapienza” and from 2000 he is Associate Professor in Electrical Engineering at the same university. He began research activity in 1982 and his interests include MHD energy conversion, low frequency electric and magnetic field computation, high frequency magnetic device modellization and non-linear electromagnetic problems related to lightning protection systems and grounding systems. These activities are described in more than 70 papers published in various international journals or presented at international conferences.

S. Lauria was born in Rome, Italy, in 1969. He received the doctor degree and the Ph.D. in electrical engineering from the University of Rome “La Sapienza” in 1996 and in 2001, respectively. In 2000 he joined the Department of Electrical Engineering of University of Rome “La Sapienza” as a Researcher. His main research interests are in power systems analysis, distributed generation, power quality and electromagnetic transients. He is a member of IEEE Power Engineering Society and of AEI (Italian Electrical Association).